Magnetoimpedance of metallic ferromagnetic wires

D.-X. Chen, J. L. Muñoz, A. Hernando, and M. Vázquez
Instituto de Magnetismo Aplicado, RENFE-UCM and Instituto de Ciencia de Materiales, CSIC, P.O. Box 155, 28230 Las Rozas, Madrid, Spain

(Received 30 June 1997; revised manuscript received 30 September 1997)

The ac impedance $Z=R+j\omega L$ of a metallic soft magnetic wire with periodic circular domains relevant to domain-wall displacements is calculated and compared with the classical model relevant to domain magnetization rotations (DMR). It is shown that the magnetoimpedance (MI) defined as the relative change of $|Z|$ with a longitudinal dc field H_{dc} at a fixed high frequency will have large values when the circular magnetization process is dominated by DMR. The single and double-peak $|Z|$ vs H_{dc} behaviors are explained and some experiments for studying MI of amorphous wires are proposed based on the model results. [S0163-1829(98)01417-9]

I. INTRODUCTION

After the discovery of giant magnetoresistance (GMR) in some materials,[1,2] the study of soft magnetic wires, tapes, and films showing an even larger magnetoimpedance (MI) has become a topic of interest owing to their possible applications as tiny field sensors.[3–12] When an ac current is applied to such a material, the impedance $Z=R+j\omega L$ across it will change sensitively with changing the longitudinal biasing field. Since the frequency of the ac current is usually high, the biasing field can also change with time rather quickly, so that the tiny field sensor also will have a quick response.

It has been shown experimentally that a large MI often occurs at frequencies as high as several MHz. With changing the dc biasing field H_{dc}, the maximum $|Z|$ can be as large as a few times of R_{dc} for amorphous wires, R_{dc} being the dc resistance. The maximum $|Z|$ can occur at $H_{dc}=0$ or $\pm H'$, H' being a nonzero constant, depending on the material and heat treatment. The major part of the $|Z|$ change occurs in an $|H_{dc}|$ range of the order of the anisotropy field.

There have been different opinions on the origin of such a MI or similar effect in soft magnetic materials. Since GMR was usually attributed to the differential scattering of conducting electrons whose spins make particular angles with the local magnetization of different scattering centers, some researchers thought that, like GMR, this effect also resulted from the electron scattering by ac current-induced domain-wall oscillations.[8,13] We have presented our different view in Refs. 14 and 7 that such an effect is the consequence of the modification of circular susceptibility by changing longitudinal field and frequency. Thus, the phenomena shoud be able to be studied in detail from the basic equations in electrodynamics.

This kind of study has been a century-long term topic for metallic materials. It has resulted in different eddy-current models for longitudinal ac permeability of metallic samples.[15–19] Such models first assumed a constant scalar dc permeability throughout the sample, which are referred to as the classical models, and then considered certain domain structures with a technical magnetization process of domain-wall displacements (DWD) or domain magnetization rotations (DMR). In the case of ac impedance, well-known quantitative models are still classical without considering domain structures.[19–21] Therefore, some current explanations of MI have to be made based on classical results with some additional modifications to include concepts of DWD, DMR, ferromagnetic resonance, and magnetic relaxation.[3,4,6,9]

In the present work, we will develop a domain model for the ac impedance of wires and give its rigorous solution. Together with the classical model, this model provides a theoretical framework within which the MI phenomena mentioned above can be better explained and some other behaviors predicted. The results of the classical model are reviewed in Sec. II before the description of the domain model in Sec. III. Based on both models, some MI phenomena are explained or predicted and some experiments are proposed in Sec. IV. Our conclusions are stated in Sec. V.

II. CLASSICAL MODEL

For the transport case of a straight wire of radius a and constant conductivity σ and scalar dc permeability μ_{dc}, the classical model gives the ratio of the ac impedance Z to the dc resistance R_{dc} as[20]

$$\frac{Z}{R_{dc}}=\frac{R+jX}{R_{dc}}=\frac{ka}{2}\frac{J_0(ka)}{J_1(ka)}, \tag{1}$$

where J_i is the ith-order Bessel function and

$$k=\sqrt{-2j}/\delta_s=\sqrt{-j}\,\theta/a, \tag{2}$$

δ_s being the classical skin depth

$$\delta_s=\sqrt{2/\sigma\mu_{dc}\omega}=\sqrt{2}a/\theta, \tag{3}$$

and θ being a parameter introduced for convenience:

$$\theta=a\sqrt{\sigma\mu_{dc}\omega}. \tag{4}$$

The low-θ^2 limit of Eq. (1) is

$$X/R_{dc}=\theta^2/8, \tag{5}$$

$$R/R_{dc}-1=\theta^4/192. \tag{6}$$

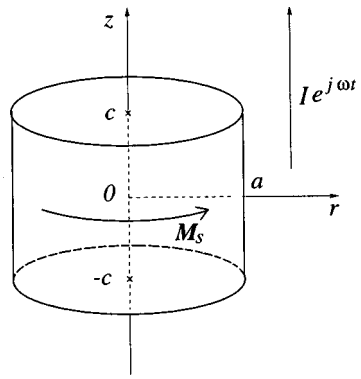

FIG. 1. A circular domain in the domain model.

The high-θ^2 limit of Eq. (1) is

$$R/R_{\rm dc}=X/R_{\rm dc}=\theta/2\sqrt{2}=a/2\delta_s. \tag{7}$$

III. A DOMAIN MODEL AND ITS SOLUTION

We assume a long straight wire of radius a and conductivity σ to be placed along the z axis. Having a circular easy direction, the magnetization $\mathbf{M}_s$ of every domain of width $2c$ is directed alternatively in the azimuth $\pm\phi$ directions, with planar disklike walls located at $z=\pm(2n+1)c$, $n=0,1,2,\ldots$. A transport current $Ie^{j\omega t}$ is applied in the z direction, which corresponds to a surface field $H_0e^{j\omega t}$ along the ϕ direction with $H_0=I/2\pi a$. The technical magnetization is carried out by DWD, with the contribution of the local differential permeability μ_0 inside the domains being neglected, as traditionally done in DWD models.[15,16] The local DWD along the z axis are assumed to be proportional to the local fields at the wall in accordance with the averaged dc permeability[22]

$$\mu_{\rm dc}=2\mu_0^2M_s^2/cq, \tag{8}$$

where q is the restoring pinning-force coefficient per unit wall area.

The total impedance is divided into two parts; the inductive external part is due to the flux outside the wire, whereas the internal one is contributed within the wire. To calculate the internal impedance along the z direction for such a periodic structure, we need to calculate for one domain in the region of $-c\leqslant z\leqslant c$ (Fig. 1) the only nonzero z component of the electrical field $E(r=a,z)e^{j\omega t}$ and average it over the side surface, and then to calculate the energy entry through this surface as will be described below.[20]

Inside the domain, the Maxwell equations and the Ohm law lead to the Laplacian equation[23]

$$\left(\frac{\partial^2}{\partial r^2}+\frac{1}{r}\frac{\partial}{\partial r}-\frac{1}{r^2}+\frac{\partial^2}{\partial z^2}\right)H(r,z)=0 \tag{9}$$

in cylindrical coordinates for the only nonzero ϕ component of magnetic field. On the boundaries, they lead to

$$H(r,z)=0\quad(r=0),\qquad H(r,z)=H_0\quad(r=a), \tag{10}$$

$$\partial H(r,z)/\partial z=k^2cH(r,z)\quad(z=\pm c), \tag{11}$$

where k is defined by Eqs. (2)–(4).

The solution to Eq. (9) under the boundary conditions (10) and (11) can be obtained by using the technique of separation of variables as follows. Since boundary condition (10) is inhomogeneous, we write

$$H(r,z)=H_1(r)+H_2(r,z), \tag{12}$$

where $H_1(r)$ satisfies Eq. (10) after changing $H(r,z)$ into $H_1(r,z)$, so that the r-boundary condition of $H_2(r,z)$ becomes homogeneous, i.e., $H_2(r,z)=0$ at $r=0$ and a. Substituting Eq. (12) in Eq. (9), we see that the equation

$$H_1(r)=H_0r/a \tag{13}$$

is the solution of $H_1(r)$ satisfying its r-boundary condition. Since $H_2(r,z)$ has a homogeneous r-boundary condition, its solution can be obtained applying the ordinary procedures of separation of variables, which can be found in many books on mathematics. Writing its particular solution as

$$H_2(r,z)=R(r)Z(z), \tag{14}$$

we have, from Eqs. (9) and (12)–(14),

$$\frac{R''}{R}+\frac{1}{r}\frac{R'}{R}-\frac{1}{r^2}=-\frac{Z''}{Z}. \tag{15}$$

Since its both sides are functions of r and z, respectively, they must be the same constant independent of r and z. Writing this constant as λ/a for convenience, Eq. (15) is separated into

$$\frac{d^2R}{d(\lambda r/a)^2}+\frac{1}{\lambda r/a}\frac{dR}{d(\lambda r/a)}+\left[1-\frac{1}{(\lambda r/a)^2}\right]R=0 \tag{16}$$

and

$$Z''-(\lambda/a)^2Z=0. \tag{17}$$

It is easy to see that Eq. (16) is the first-order Bessel equation, and its eigensolution for the homogeneous boundary condition mentioned above is

$$R_n(r)=J_1(\lambda_nr/a), \tag{18}$$

where J_i is the ith-order Bessel function and λ_n is the nonzero value of the argument of J_1 at the nth zero point, namely, $J_1(\lambda_n)=0$.

Replacing λ in Eq. (17) by λ_n, its general solution becomes

$$Z(z)=A_n\cosh(\lambda_nz/a), \tag{19}$$

where the coefficient A_n should be determined by boundary condition (11). Since $J_1(\lambda_nr/a)$, $n=1,2,\ldots$, form an orthogonal complete function system, the general solution of $H_2(r,z)$ turns out to be

$$H_2(r,z)=\sum_{n=1}^{\infty}A_n\cosh(\lambda_nz/a)J_1(\lambda_nr/a), \tag{20}$$

and Eq. (13) can be expanded as

$$H_1(r)=2H_0\sum_{n=1}^{\infty}J_1(\lambda_nr/a)/J_2(\lambda_n). \tag{21}$$

Thus,

$$\frac{H(r,z)}{H_0}=\frac{r}{a}+\sum_{n=1}^{\infty}A_n\cosh\frac{\lambda_n z}{a}J_1\left(\frac{\lambda_n r}{a}\right)$$

$$=\sum_{n=1}^{\infty}\left[\frac{2}{J_2(\lambda_n)}+A_n\cosh\frac{\lambda_n z}{a}J_1\left(\frac{\lambda_n r}{a}\right)\right]. \quad (22)$$

Substituting Eq. (22) in Eq. (11), we obtain

$$A_n=\frac{2k^2ac}{\lambda_n J_2(\lambda_n)}\left[\lambda_n\sinh\frac{\lambda_n c}{a}-k^2ac\cosh\frac{\lambda_n c}{a}\right]^{-1}. \quad (23)$$

From the Ampere law and the Ohm law, the only nonzero z component of the electrical field, $E(r,z)e^{j\omega t}$, on the side surface is calculated as

$$\frac{a\sigma}{H_0}E(r=a,z)=2-\sum_{n=1}^{\infty}A_n\lambda_n J_2(\lambda_n)\cosh(\lambda_n z/a). \quad (24)$$

The internal impedance of the domain should be derived from the energetical definitions of resistance and inductance.[20] For this, we calculate the energy entering the domain per second through the side surface, $P=2\pi aH_0\int_{-c}^{c}E(r=a,z)dz$, and write

$$Z=R+jX=P/I^2. \quad (25)$$

Thus, it turns out that

$$\frac{R}{R_{\rm dc}}=1+\frac{\theta^4 c}{a}\sum_{n=1}^{\infty}\frac{1}{\lambda_n}\left[\lambda_n^2\tanh\frac{\lambda_n c}{a}+\frac{\theta^4c^2}{a^2}\coth\frac{\lambda_n c}{a}\right]^{-1}, \quad (26)$$

$$\frac{X}{R_{\rm dc}}=\theta^2\sum_{n=1}^{\infty}\left[\lambda_n^2+\frac{\theta^4c^2}{a^2}\coth^2\frac{\lambda_n c}{a}\right]^{-1}. \quad (27)$$

$R/R_{\rm dc}-1$, $X/R_{\rm dc}$, and $|Z|/R_{\rm dc}$ as functions of θ^2 are computed using Eqs. (26) and (27) for $c/a=0.01$, 0.1, 1, 10, and 100. The results are plotted in Fig. 2. We note that the convergence of the sums in Eqs. (26) and (27) is very slow, and we have taken the number of terms up to 10^7 to get satisfactory results.

Since when $c/a\ll 1$ the domain walls are very densely placed in the wire, the results for $c/a=0.01$ shown in Fig. 2 coincide well with those of the classical model. Thus, the low-c/a limit of the domain model can also be called the classical limit.

We see from Fig. 2(b) that at low θ^2, the $X/R_{\rm dc}$ curves for all values of c/a collapse into one, which is also the low-θ^2 limit of the classical model expressed by Eq. (5). As seen in Fig. 2(a), the low-θ^2 behavior of $R/R_{\rm dc}$ evolves from the classical limit as

$$R/R_{\rm dc}-1=\eta\theta^4/192, \quad (28)$$

where η is the anomaly factor for eddy-current loss, which equals 1 at $c\ll a$, but approaches

$$\eta=4.37c/a \quad (29)$$

if $c/a>1$.

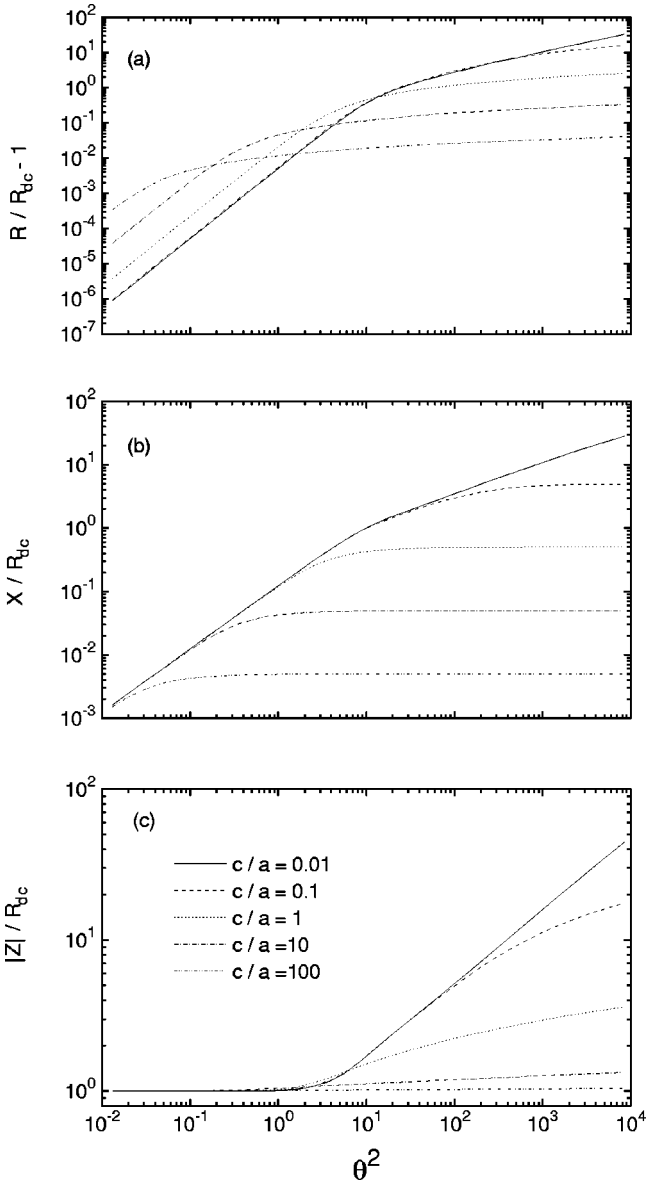

FIG. 2. $R/R_{\rm dc}-1$ (a), $X/R_{\rm dc}$ (b), and $|Z|/R_{\rm dc}$ (c) as functions of θ^2 for $c/a=0.01$, 0.1, 1, 10, and 100.

At high θ^2, we have $X/R_{\rm dc}=a/2c$ and $R/R_{\rm dc}$ increases steadily with increasing θ^2, being $\sim a/2c$ at $\theta^2=100$. As a result, the $|Z|/R_{\rm dc}$ change with increasing θ^2 shown in Fig. 2(c) has the following features: It increases from 1 for all cases. An appreciable change occurs when $\theta^2>1$ and $a/c<10$. The maximum change increases with decreasing c/a up to the maximum one, which is $\propto\theta$ and occurs at $c/a=0.01$ or the classical limit.

IV. MAGNETOIMPEDANCE

A. Direct prediction of the domain model

MI is defined from the change in Z at a given ω resulting from the change in a biasing dc field $H_{\rm dc}$. Therefore, it takes place when $\mu_{\rm dc}$, domain structure, and magnetization process change with $H_{\rm dc}$. Before considering how they change with $H_{\rm dc}$, we give a direct prediction of our model on MI as follows. A large MI occurs at high θ^2 and $c/a\leqslant 0.1$. For

$c/a \leqslant 0.01$ or the classical limit, the maximum $|Z|$ change can be more than 10 times when θ^2 changes for 100 times. If assuming such a θ^2 change to be between 0.7 and 70 or between 7 and 700, which corresponds to a change of μ_{dc}/μ_0 between 100 and 10 000, we calculate the required working frequency $f=\omega/2\pi$ from Eq. (4). Using $\sigma=0.8\ \mathrm{M\Omega^{-1}\,m^{-1}}$ and $2a=0.124$ mm for a zero-magnetostrictive amorphous wire,[7] the result is $f=0.31$ MHz or 3.1 MHz with a 4 or 10 times of $|Z|$ change. Thus, the typical working frequency for a large MI should be ~ 1 MH or greater, in consistency with the experimental data.[3–6,8]

B. Domain structures of amorphous wires

We now comment on the domain model used in our calculations. In the experiments of MI, most samples were obtained by rapid quenching. In rapidly quenched wires, different domain structures were observed for different materials.[24–29] For iron based wires with a large positive saturation magnetostriction λ_s, the quenched-in stress distribution results in a longitudinal easy axis in the cylindrical core and somehow radial easy axes in the tubular shell. In the initial or remanent state, there are an inner cylindrical domain with longitudinal magnetization and an outer region where magnetizations are basically radial with complicated closure domains. For cobalt based wires with modest negative λ_s, the quenched-in stresses may make the surface anisotropy be circular and the inner anisotropy be perpendicular, forming a domain structure consisting of circular domains. For wires with nearly zero λ_s, other induced anisotropies may overcome the stress anisotropy, and the domain structure becomes not well defined.

Our domain model is made based on the observation of domain structures of cobalt based amorphous wires. However, like the relevance of Pry-Bean's and Polivanov's bar-domain models to the ac permeability of metallic soft-magnetic tapes with complex domain structures,[15–18] its results should be generally valid for all wires whose surface circular technical magnetization is dominated by DWD. Since a large MI requires a large μ_{dc}, the model should be preferably used for wires with small λ_s.

In the domain model, the domain wall thickness is assumed to be zero. This is not realistic. The wall thickness of nearly zero λ_s amorphous materials can be as large as a few micrometers.[30] Thus, for a wire of $2a \sim 0.1$ mm, $c/a=0.01$ corresponds to a case of domain width being smaller than the wall thickness. Being the classical limit, the results of $c/a=0.01$ can be used for DMR if the static domain magnetizations $\mathbf{M}_s$'s are along the wire and there is only a circular component of $\mathbf{M}_s$ rotations in small circular fields.

C. Single- and double-peak magnetoimpedance

In the following, we discuss two types of MI based on our results. If intrinsic or induced anisotropies are very small $(K_u \approx 0)$, most domains should be large with $\mathbf{M}_s$'s along the wire at $H_{dc}=0$ owing to the shape anisotropy. In this case, the circular μ_{dc} will result from DMR and be very large, so that the $|Z|/R_{dc}$ at $H_{dc}=0$ is very large at a not very high ω according to the results at the classical limit in Fig. 2. At a nonzero $|H_{dc}|$, the circular $\mu_{dc}/\mu_0 \approx M_s/H_{dc}$ owing to the unidirectional magnetostatic anisotropy.[31] Thus, θ and so $|Z|$ decrease with increasing $|H_{dc}|$ as $|H_{dc}|^{-1/2}$ according to Eq. (4) and Fig. 2 at a sufficiently large ω, showing a typical single-peak MI.

The second type of MI occurs when there is a dominating circular anisotropy with anisotropy field H_k (see Sec. IV E). The initial domain structure may be like the modeled one. In this case at $H_{dc}=0$, a circular ac field does not exert a torque on $\mathbf{M}_s$'s and the μ_{dc} at $H_{dc}=0$ controlled by DWD cannot be very large, so that θ^2 is quite small at a not very high ω. The increase of $|H_{dc}|$ will increase the domain sizes and rotate $\mathbf{M}_s$'s away from the circular directions, so that DMR take place when ac current is applied. The DMR μ_{dc} increases with increasing $|H_{dc}|$ to a maximum at $|H_{dc}|=H_k$, where $\mathbf{M}_s$ starts to be along the axial direction and the effective anisotropy field $|H_{dc}-H_k|$ becomes ideally 0. Upon further increasing $|H_{dc}|$, we have the DMR $\mu_{dc}/\mu_0 \approx M_s/(|H_{dc}|-H_k)$.[31] Thus, at a sufficiently large ω with increasing $|H_{dc}|$, $|Z|$ increases until $|H_{dc}|=H_k$ and then decreases as $(|H_{dc}|-H_k)^{-1/2}$, showing a double-peak MI.

D. Magnetoimpedance of amorphous wires

For amorphous wires with nearly-zero λ_s, the small anisotropies required by the single-peak MI can be realized for materials whose crystallization temperature T_{cry} is higher than the Curie temperature T_c for more than 100 K after annealing between T_c and T_{cry} (e.g., at $T_a=T_{cry}-80$ K) followed by water quenching.[32,33]

If the wire has a longitudinal anisotropy of constant K_u, which can be achieved by a longitudinal field annealing or the application of a large tension if $\lambda_s>0$, there will be essentially a single longitudinal domain. In this case, the circular magnetization will be carried out by DMR and the maximum $|Z|$ should occur at $H_{dc}=0$, calculated by $\mu_{dc} \approx \mu_0 M_s^2/2K_u$. At ω higher than that for the case of $K_u \approx 0$, $|Z|$ decreases with H_{dc} as $(|H_{dc}|+2K_u/\mu_0 M_s)^{-1/2}$, showing also a single-peak MI.

For amorphous wires with nearly-zero λ_s, the perpendicular anisotropy required by the double-peak MI can be induced by current annealing below T_c or more efficiently, tension annealing above T_c.[34–36] If $\lambda_s<0$, the application of a large tension also gives such an anisotropy.

In the double-peak case at low ω, there can be additional $|Z|$ peaks occurring at $|H_{dc}|<H_k$.[11] Such peaks should be the consequence of DWD. A few domain wall jumps at H_{dc} close to the coercivity can result in a high μ_{dc} so that a $|Z|$ peak occurs.

A large MI requires a large maximum $|Z|$ for both cases. Since a distribution of anisotropies will limit the reached maximum μ_{dc}, the most important condition for the sample is the high uniformity in anisotropy. Thus, in order to increase MI, our main effort should be put on looking for a proper annealing condition to realize such a magnetic uniformity.

E. Current amplitude dependence

In both the classical and domain models, μ_{dc} is assumed to be constant. For ferromagnetic samples, this is valid for

small ac current so that circular dc magnetization is reversible. When the amplitude of the ac current, $I_{\max}$, is increased, irreversible dc magnetization gives rise to a greater effective $\mu_{\rm dc}$. Thus, a greater maximum $|Z|$ are expected at a greater $I_{\max}$.

For double-peak MI, the $|H_{\rm dc}|$ at which $|Z|$ takes maximum should decrease with increasing $I_{\max}$. In this case when $I_{\max}$ is small, the $|Z|$-peak $|H_{\rm dc}|$ results from the compensation between $H_{\rm dc}$ and H_k. The anisotropy field H_k is calculated from small angle magnetization rotation away from the easy direction. If the angle amplitude is α_m, such a compensation can be estimated by comparison of average torques exerted on $\mathbf{M}_s$ from the anisotropy and $H_{\rm dc}$. Assuming the anisotropy energy $E_k = K_u \cos^2 \alpha$, then the angular averaged torque owing to it is $T_k = -K_u(1-\cos 2\alpha_m)/2\alpha_m$. The angular averaged torque owing to the magnetostatic energy $E_m = \mu_0 M_s H_{\rm dc}(1-\cos\alpha)$ is $T_m = \mu_0 H_{\rm dc}(1-\cos\alpha_m)/\alpha_m$. At the compensation, we have $T_k + T_m = 0$, so that the compensation field

$$H_{\rm dc,comp} = \frac{K_u}{2\mu_0 M_s}\,\frac{1-\cos 2\alpha_m}{1-\cos\alpha_m}. \tag{30}$$

From this equation, we see that if with increasing $I_{\max}$ α_m increases from 0 to $\pi/2$, $H_{\rm dc,comp}$ will decrease from $H_k = 2K_u/\mu_0 M_s$ to $H_k/2$.

F. Magnetoimpedance at very high frequencies

In the above, the explanations of MI are made in terms of eddy-current models. Such models are vadid for frequencies below about 100 MHz, since the Polivanov model and the classical model have been successfully used for explaining the ac permeability of many metallic soft-magnetic tapes at frequencies up to 30 MHz.[37–39] If a high frequency leads to a skin-depth comparable with the exchange length, both the classical and the flexible-wall domain models do not work. Actually, ferromagnetic resonance occurs at $f \sim 1$ GHz, which becomes the main effect responsible for the Z change.[12]

V. CONCLUSION

For understanding the MI in metallic soft-magnetic wires, we have calculated the ac impedance of a wire of diameter $2a$ with periodic circular domains of width $2c$. Together with the classical model, whose results are identical to the low-c/a limit, the results are used for the contributions of domain-wall displacements (DWD) and domain magnetization rotations (DMR). The main conclusions are as follows. For typical amorphous wires, a large MI occurs at frequencies greater than MHz where skin effects are pronounced. A large MI requires DMR to be the dominating circular technical magnetization mechanism. DWD can give an appreciable contribution to MI if c/a is not very large. For the single-peak MI, a large maximum impedance at $H_{\rm dc}=0$ requires uniform and small anisotropies; for double-peak MI, it requires a uniform perpendicular anisotropy. These rules can serve as a guide for a proper choice of materials and heat-treatments to realize large MI. The impedance decrease at high $H_{\rm dc}$ is caused by DMR on which the restoring torque is dominated by magnetostatic energy. Our work may be useful for experimentalists who have found many other phenomena on MI.

[1] M. N. Baibich, J. M. Broto, A. Fert, F. Nguyen Van Dau, F. Petroff, P. Etienne, G. Creuzet, A. Friederich, and J. Chazelas, Phys. Rev. Lett. **61**, 2472 (1988).

[2] R. L. White, IEEE Trans. Magn. **28**, 2482 (1992).

[3] R. S. Beach and A. E. Berkowitz, Appl. Phys. Lett. **64**, 3652 (1994); J. Appl. Phys. **76**, 6209 (1994).

[4] L. V. Panina and K. Mohri, Appl. Phys. Lett. **65**, 1189 (1994).

[5] L. V. Panina, K. Mohri, K. Bushida, and M. Noda, J. Appl. Phys. **76**, 6198 (1994).

[6] L. V. Panina, K. Mohri, T. Uchiyama, K. Bushida, and M. Noda, in *Proceedings of the 4th International Workshop on Non-Crystalline Solids*, edited by M. Vázquez and A. Hernando (World Scientific, Singapore, 1994), p. 461.

[7] J. Velázquez, M. Vázquez, D.-X. Chen, and A. Hernando, Phys. Rev. B **50**, 16 737 (1994).

[8] F. L. A. Machado, C. S. Martins, and S. M. Rezende, Phys. Rev. B **51**, 3926 (1995).

[9] L. V. Panina and K. Mohri, J. Magn. Magn. Mater. **157/158**, 137 (1996).

[10] M. Tejedor, B. Hernando, M. L. Sánches, and A. García-Arribas, J. Magn. Magn. Mater. **157/158**, 141 (1996).

[11] R. L. Sommer and C. L. Chien, J. Appl. Phys. **79**, 5139 (1996).

[12] D. Ménard, M. Britel, P. Ciureanu, A. Yelon, V. P. Paramonov, A. S. Antonov, P. Rudkowski, and J. O. Ström-Olsen, J. Appl. Phys. **81**, 4032 (1997).

[13] K. Mandal and S. K. Ghatak, Phys. Rev. B **47**, 14 233 (1993).

[14] M. Vázquez, J. Velázquez, and D.-X. Chen, Phys. Rev. B **51**, 652 (1995).

[15] R. H. Pry and C. P. Bean, J. Appl. Phys. **29**, 532 (1958).

[16] K. M. Polivanov, Izv. Akad. Nauk SSSR, Ser. Fiz. **16**, 446 (1952).

[17] J. E. L. Bishop, J. Phys. D **4**, 1235 (1971).

[18] D.-X. Chen and J. L. Muñoz, IEEE Trans. Magn. **33**, 2227 (1997).

[19] R. M. Bozorth, *Ferromagnetism* (Van Nostrand, New York, 1951), p. 776.

[20] L. D. Landau, E. M. Lifshitz, and L. P. Pitaevskii, *Electrodynamics of Continuous Media* (Butterworth-Heinenann, Washington, DC, 1995), p. 210.

[21] P. M. Perry, IEEE Trans. Power Appar. Syst. **PAS-98**, 116 (1979).

[22] S. Chikazumi, *Physics of Magnetism* (Wiley, New York, 1964), p. 264.

[23] From Maxwell's equations and Ohm's law, $\nabla\times\mathbf{E} = -\partial\mathbf{B}/\partial t$ and $\nabla\times\mathbf{H} = \sigma\mathbf{E}$, we have $\nabla\times\nabla\times\mathbf{H} + j\omega\sigma\mu\mathbf{H} = 0$, which leads to $\nabla^2\mathbf{H} - j\omega\sigma\mu\mathbf{H} = 0$ since $\nabla\cdot\mathbf{H} = 0$. In the domain model, we have neglected μ inside the domain, i.e., $\mu = 0$, so that $\nabla^2\mathbf{H} = 0$, which is written Eq. (9) in cylindrical coordinates.

[24] H. Kawamura, K. Mohri, and J. Yamasaki, Jpn. J. Appl. Magn. Soc. **12**, 249 (1988).

[25] J. Yamasaki, Jpn. J. Appl. Magn. Soc. **16**, 14 (1992).

[26] T. Reininger, H. Kronmüller, C. Gómez-Polo, and M. Vázquez, J. Appl. Phys. **73**, 5357 (1993).

[27] D. Atkinson, M. R. J. Gibbs, P. T. Squire, and Q. Pankhurst, J. Magn. Magn. Mater. **131**, 19 (1994).

[28] H. Theuss, B. Hofmann, C. Gómez-Polo, M. Vázquez, and H. Kronmüller, J. Magn. Magn. Mater. **145**, 165 (1995).

[29] M. Vázquez, C. Gómez-Polo, H. Theuss, and H. Kronmüller, J. Magn. Magn. Mater. **164**, 319 (1996).

[30] D.-X. Chen, C. F. Conde, H. Miranda, and A. Conde, J. Magn. Magn. Mater. **111**, 135 (1992).

[31] Without considering other anisotropies, $\mathbf{M}_s$ should be along the vectorial sum of the axial $\mathbf{H}_{\rm dc}$ and the circular field $\mathbf{H}_{\rm circ}$. Thus, for small angle of rotations of $\mathbf{M}_s$ away from the axis, we have $M_{\rm circ}/M_s \approx H_{\rm circ}/H_{\rm dc}$, or $\mu_{\rm dc}/\mu_0 \approx M_{\rm circ}/H_{\rm circ} \approx M_s/|H_{\rm dc}|$. Similarly, we have $\mu_{\rm dc}/\mu_0 \approx M_s/(|H_{\rm dc}|-H_k)$ if a circular anisotropy field H_k is considered.

[32] D.-X. Chen, Acta Metall. Sin. **19**, A422 (1983).

[33] P. T. Squire, M. R. J. Gibbs, and A. P. Thomas, J. Magn. Magn. Mater. **83**, 179 (1990).

[34] O. V. Nielsen and H. J. V. Nielsen, Solid State Commun. **35**, 281 (1980); J. Magn. Magn. Mater. **22**, 21 (1980).

[35] H. R. Hilzinger, in *Proceedings of the 4th International Conference Rapid Quenched Metals*, edited by T. Masumoto and K. Susuki (Japan Institute of Metals, Sendai, 1982), p. 791.

[36] D.-X. Chen and L.-Z. Tai, Chin. Phys. Lett. **2**, 71 (1985); D.-X. Chen, J. Appl. Phys. **61**, 378 (1987).

[37] P. G. Collar, E. W. Lee, and J. E. L. Bishop, Br. J. Appl. Phys., J. Phys. D **2**, 1353 (1969).

[38] J. E. L. Bishop, P. G. Collar, and E. W. Lee, Br. J. Appl. Phys., J. Phys. D **3**, 1586 (1970).

[39] J. E. L. Bishop, P. G. Collar, and E. W. Lee, Br. J. Appl. Phys., J. Phys. D **4**, 1221 (1971).